IEEE Access
Multidisciplinary : Rapid Review : Open Access Journal

Received February 27, 2019, accepted March 13, 2019, date of publication March 21, 2019, date of current version April 5, 2019.

Digital Object Identifier 10.1109/ACCESS.2019.2906779

Distribution Network Security Situation Awareness Method Based on Security Distance

JUN XIAO, (Member, IEEE), BAOQIANG ZHANG, AND FENGZHANG LUO, (Member, IEEE)
Key Laboratory of Smart Grid of Ministry of Education, Tianjin University, Tianjin 300072, China

Corresponding author: Fengzhang Luo (luofengzhang@tju.edu.cn)

This work was supported in part by the National Key Research and Development Program of China under Grant 2016YFB0900100, and in part by the National Natural Science Foundation of China under Grant 51877144.

ABSTRACT Situation awareness (SA) refers to the process of perception, comprehension, and state projection of the system, elements, and environmental factors within a volume of time and space. The security assessment is an important part of SA for distribution networks. In this paper, the distribution system security region (DSSR) is used for SA for the first time, and a security SA method based on security distance (SD) is proposed. First, based on the existing DSSR, which is defined as the set of all operating points (OPs) satisfying $N-1$ security criterion, this paper supplements the $N-0$ DSSR satisfying normal operating constraints. Second, calculate SDs between the OP and security boundaries to determine whether an OP is secure. If one is secure, its SDs can give the security margin; while if one is insecure, its SDs can give the degree of insecurity and the fault, or the overload components can be recognized via the cross security boundary analysis. The situation comprehension for the distribution network security is realized through the above-mentioned information. Third, the security level of distribution networks in the future can be predicted by the trends of SDs. Finally, the feasibility and effectiveness of the proposed method are verified by an actual distribution network case.

INDEX TERMS Distribution system security region (DSSR), security assessment, security distance, situation awareness (SA).

NOMENCLATURE

$\boldsymbol{\Omega}_{\mathrm{DSSR}}$	DSSR
$\boldsymbol{\Omega}_{\mathrm{DSSR0}}$	DSSR0
$\partial\boldsymbol{\Omega}_{\mathrm{DSSR}}$	Boundaries of DSSR
$\partial\boldsymbol{\Omega}_{\mathrm{DSSR0}}$	Boundaries of DSSR0
β_{i}	The i^{th} DSSR boundary
β_i^0	The i^{th} DSSR0 boundary
$\boldsymbol{\Theta}$	State space
$\boldsymbol{W}$	Operating point
$\boldsymbol{V}$	Voltage amplitude
$\boldsymbol{\theta}$	Phase angle
c_i	The capacity of component i
S_i	The apparent power of the bus i
SD_{i}	Security distance in DSSR in the direction of feeder i
SD_i^0	Security distance in DSSR0 in the direction of feeder i
$\alpha_{k,j}$	The coefficient of S_j in the hyperplane k.

The associate editor coordinating the review of this manuscript and approving it for publication was Md. Jahangir Hossain.

I. INTRODUCTION

Distribution networks play a significant role in power systems, of which the secure and reliable operations are critical [1]. Situation awareness (SA) is considered to be an important analysis technology supporting the operation of distribution networks. The concept of SA is firstly proposed in the domains of aviation and military [2], which is defined as the perception of the elements in an environment within a volume of time and space, the comprehension of their meaning, and the projection of their status in the near future. Before long, this concept and its implications have been widely used in other domains, including electric power systems [3]. The process of SA for distribution networks can be divided into three separate levels [4]: 1) Perception: acquiring the information related to key elements of a distribution network. 2) Comprehension: analyzing what the perceived data means and forming the assessment of the grid state. 3) Projection: predicting the future behavior of system components based on their current state and on the perceived information. Dispatchers can develop a set of strategies and responses to events, which contributes to the prevention of undesirable situations.

With the development and application of advanced metering infrastructure (AMI) and big data analysis, it is possible to extract the data features from extensive distribution network information, which lays the foundation for SA. The framework and attention areas of SA in distribution networks are proposed in [3] and [4]. AMI is used to perceive the health and status of components in distribution networks [5]. Based on the big data analysis of the distribution network, fuzzy cluster based analytical method, game theory and reinforcement learning are integrated to improve fault identification ratio in [6]. Two indices including network total active power loss and node voltage variations are proposed to reflect the distribution networks operation state in [7]. Several research works have been devoted to SA for distribution networks, and most of them are focus on $N-0$ security in normal operation [3]–[7], rarely involving $N-1$ security. However, for an actual central city distribution network, the common security issues that occur during the peak period of the summer power consumption are capacity violation issues. Due to the rapid growth of load over the $N-1$ security limit without warning, the normal operation limit would be exceeded, and even the serious consequences of load shedding would occur. Therefore, it is very necessary to consider $N-1$ security in the SA for distribution networks, which can prompt the dispatchers to take preventive control measures to avoid the problem from continuing to deteriorate.

The most commonly used method for evaluating the security of distribution networks is via commercial simulation packages [8], which is limited in application to real-time manner due to the high nonlinearity and high dimensionality of large scale distribution networks. Hence, there is an urgent need for a fast, accurate tool to evaluate the security level and to provide instructive results to help dispatchers take preventive measures in advance.

The distribution system security region (DSSR) theory proposed in recent years [9]–[12] has been proved to have good prospects in online monitoring of distribution network operation. DSSR is the maximum operational range in its state space for a distribution network satisfying $N-1$ security criterion, of which the boundaries can be calculated and observed by simulation approach [13]. The existence of DSSR is proved by mathematical deduction [14] and the practice in a real distribution network [15], respectively. In [15], comparison between the DSSR theoretical results and the real results from the dispatchers shows that DSSR boundary calculation results match the actual situation of the real case.

DSSR can provide entire information of the operation states. Hence, we only need to check whether the given operating point (OP) lies inside the region to determine its security. Moreover, by calculating the distance from an OP to security boundaries [16], [17], we are able to assess its security margins [18]. Since the security distance (SD) can give an overall picture of the current situation, its advantages in real-time monitoring are expected to be applied in SA. In this paper, DSSR is applied to SA for the first time, and SD is used to evaluate the OP's security or insecurity degree of the distribution network, so as to realize situation comprehension and situation projection.

The rest of this paper is organized as follows. In Section II, the $N-0/N-1$ security, DSSR and SD for distribution networks are briefly introduced. Section III provides the framework and method of SA based on SD. The evaluations of the proposed method are illustrated in Section IV. Section V concludes this paper.

II. PRELIMINARY CONCEPTS

A. $N-0/N-1$ SECURITY FOR DISTRIBUTION NETWORKS

The distribution networks under normal operation state should be able to maintain stable operation and continuous power supplies, which is usually called $N-0$ security. If a distribution network can maintain reliable power supplies to those areas without a fault under any single contingency, we call it $N-1$ security [8]. A distribution network is $N-1$ secure, meaning that any fault in the primary feeders or substation transformers will lead to a service interruption of the faulted section only. Hence, the service to the upstream of a faulted feeder section will be restored after opening the first switchable component upstream to the faulted section, and the service to the downstream will be restored through back feed via closing a normally open tie switch. A simple example as shown in Fig. 1 is used to explain the $N-0/N-1$ security for distribution networks.

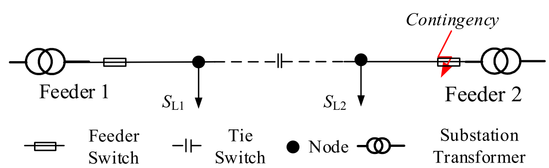

FIGURE 1. $N-0/N-1$ **security for distribution networks.**

In Fig. 1, when the network is under normal operation state, the tie switch is open, load L1 and L2 are supplied by feeder 1 and 2, respectively. The feeder capacity constraints should be satisfied

$$S_{L1} \le c_1, \quad S_{L2} \le c_2 \tag{1}$$

where c_1 is the capacity of feeder 1,c_2 is the capacity of feeder 2. If the inequalities above are satisfied, the system is $N-0$ secure. When a single contingency occurs at the outlet of feeder 2, the tie switch would be closed and both the load L1 and L2 are supplied by feeder 1. Therefore, the feeder 1 capacity constraint should be formulated as

$$S_{L1} + S_{L2} \le c_1 \tag{2}$$

If the inequality above is satisfied, the system is $N-1$ secure for this single contingency.

B. DISTRIBUTION SYSTEM SECURITY REGION

1) OPERATING POINT

Operating point (OP), denoted by $\boldsymbol{W}$, is defined as the vector of the apparent power of all the non-slack feeders. For a distribution network with n non-slack feeders,

$$\boldsymbol{W} = (S_1, S_2, \ldots, S_i, \ldots, S_n)^T \tag{3}$$

where S_i is the apparent power of feeder i. In the actual operation of distribution networks, the nodes power flow changes continuously in a certain range, which can be formulated as:

$$\forall 1 \leq i \leq n, \quad \exists S_{i,max} > 0,\ 0 \leq S_i \leq S_{i,max} \tag{4}$$

where the $S_{i,\max}$ is the upper limit of S_i.

2) DSSR AND DSSR0 MODEL

DSSR is defined as the set of all OPs satisfying $N-1$ security criterion [9], formulated as:

$$\boldsymbol{\Omega}_{\text{DSSR}} = \{\boldsymbol{W} \in \boldsymbol{\Theta} | f(\boldsymbol{V}, \boldsymbol{\theta}) = \boldsymbol{W}, g_{N-1}(\boldsymbol{W}) \leq 0\} \tag{5}$$

where $\boldsymbol{\Theta}$ is the state space,$f(\boldsymbol{V}, \boldsymbol{\theta}) = \boldsymbol{W}$ are the power flow equations, $g_{N-1}(\boldsymbol{W}) \leq 0$ are the security constraints after $N-1$ contingency. As a distinction, we name the set of OPs satisfying $N-0$ security criterion as DSSR0, denoted by $\boldsymbol{\Omega}_{\text{DSSR0}}$. The detailed AC-Flow models of DSSR and DSSR0 are illustrated in Appendix A.

3) SECURITY BOUNDARY

Security constraints change into security boundaries when becoming equations. Some of AC-Flow security boundaries can be simulated by OpenDSS, and they can be approximately expressed by several hyperplanes in the vector space using DC power flow [13], named linear security boundaries in this paper and formulated as

$$\sum_{j=1,\ldots,n} \alpha_{k,j} S_j = 1, \quad S_j \in \boldsymbol{W}, \ \boldsymbol{W} \in \boldsymbol{\Omega}_{DSSR} or \boldsymbol{\Omega}_{DSSR0} \tag{6}$$

where $\alpha_{k,j}$ is the coefficient of S_j in the hyperplane k. In addition, the boundary from a $N-0$ security constraint is termed as $N-0$ security boundary while that from a $N-1$ security constraint is termed as $N-1$ security boundary.

C. DISTRIBUTION SYSTEM SECURITY DISTANCE

SD for distribution networks is defined as the distance from an OP to security boundaries [9]. It can describe the security margin precisely. Two kinds of SDs are proposed in [16], which are geometric SD and feeder SD, respectively. In this paper, we calculate SD by the way of feeder SD because it is more practical than geometric SD to represent the increasable load of feeders. Feeder SD is essentially a state distance. It is state distance (state variables variation) that makes an operating point operate to another operating point. For instance, load power of some nodes needs to reduce in order to control operating points back to security state. The sum of absolute value of load power variation is a kind of 'cost'.

SD in the direction of feeder i is calculated as:

$$SD_i = \min_{\beta_k \in \Omega_{(i)}} \sum_{j=1}^{n} \left| S_j - S_{j,\beta_k} \right| \tag{7}$$

where β_k.is the boundary which an OP will cross over in the direction of feeder i; $\boldsymbol{\Omega}_i$ is the set of β_k. The absolute value of SD means the maximum increasable load or the minimum load shedding on feeder i, or on the feeders of which the ID appearing in the expression of the nearest boundary to the OP in the direction of feeder i (the closely related feeders of feeder i for short in the later section) [19].

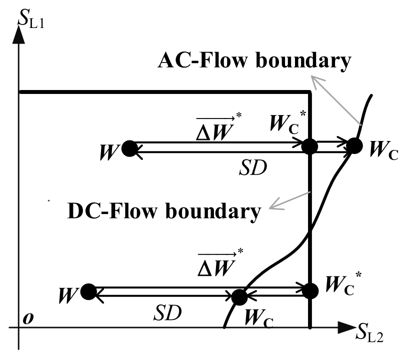

FIGURE 2. The two-step method for calculating SD.

According to the definition of SD, it is necessary to express each security boundary first. However, accurate analytical expressions of security boundary based on AC-Flow are difficult to obtain now. Therefore, this paper uses DC-Flow model to obtain approximate boundaries in the first step and then calculate SDs based AC-Flow in the second step. The two-step method is shown in Fig. 2. Step 1: take $\boldsymbol{W}$ as a starting point, then calculate corresponding cross-boundary point $\boldsymbol{W}_{\text{C}}^*$ on DC-Flow boundary and cross-boundary displacement $\overrightarrow{\boldsymbol{\Delta W}}^*$; Step 2: take $\boldsymbol{W}_{\text{C}}^*$ as a starting point, according to the positive or negative direction of $\overrightarrow{\boldsymbol{\Delta W}}^*$, find cross-boundary point $\boldsymbol{W}_{\text{C}}$ on the AC-Flow boundary, then calculate the accurate SD.

III. SD-BASED SITUATION AWARENESS

A. RELATIONSHIP BETWEEN SA AND SECURITY FOR DISTRIBUTION NETWORKS

Security is very important for distribution networks. It relates to the current system state and the fault state that may occur in the future. The distribution network security analysis mainly includes the following steps. First, it is necessary to collect as much data as possible about the distribution network, including the power flow of the feeders, the voltage amplitude, the phase angle of the nodes, the switching state, etc. Second, based on the collected data, the current state of the system can be evaluated by calculating the security indicator, so that the dispatchers can learn the current system state. Third, according to the existing data, the operation of the grid in the future is predicted, such as the load forecasting, which provides a reference for the follow-up operation of dispatchers. It can be seen that the distribution network security analysis process conforms to the definition of three stages of SA. Therefore, security is the basic content of SA for distribution networks.

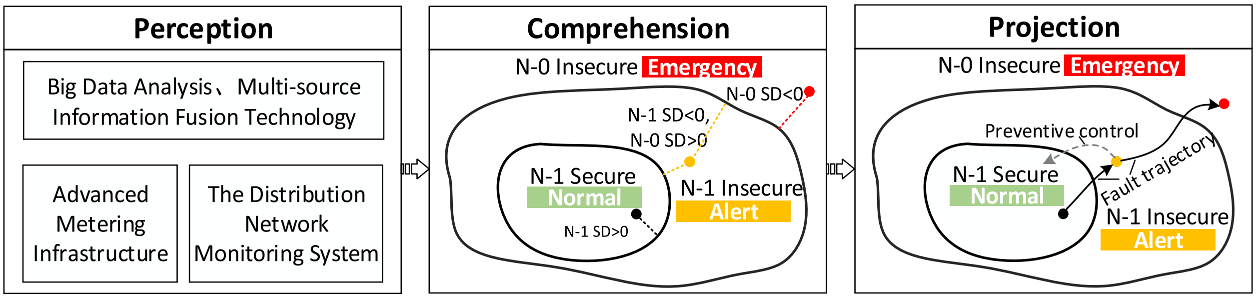

FIGURE 3. The framework of SA for distribution networks based on SD.

B. FRAMEWORK OF SA BASED ON SD

The SD-based SA framework for distribution networks is shown in Fig. 3.

The development and application of AMI and big data analysis lay the foundation for SA [5], [6]. Therefore, this paper focuses on comprehension and projection of SA, and the main idea is as follows.

(1) Security boundaries can be calculated offline firstly by using the DC power flow [9] to make a foundation for the calculation of SD.

(2) Calculate SDs by using the two-step method shown in Section 2.3. If an OP is secure, its SDs can give the degree of security; while if one is insecure, its SDs can give the degree of insecurity. Via the analysis of cross security boundary, we can know the fault or overload components [21].

(3) For the situation projection of a distribution network, this paper proposes to predict the security level in the future by the trends of SDs, with which the dispatchers can take necessary preventive measures.

C. SD-BASED COMPREHENSION

Both $N-0$ SDs and $N-1$ SDs can quantify the security margin, we can judge whether an OP satisfies $N-0/N-1$ security by $N-0/N-1$ SDs, respectively. In Table 1, we take $N-1$ SD as an example to show how to realize situation comprehension by it.

TABLE 1. Situation comprehension results obtained from $N-1$ sds condition.

N-1 SDs condition	Situation comprehension results
N-1 $SD_i \geq 0$	(1) The maximum increasable load value SD_i in the direction of feeder i.
$\forall\ i=1,\ldots,m$, N-1 $SD_i \geq 0$	(1) The OP satisfies N-1 security. (2) The maximum increasable load value SD_i in the direction of any feeder i.
$\exists\ i$, N-1 $SD_i<0$	(1) The OP does not satisfy N-1 security. (2) The minimum load shedding value $\|SD_i\|$ in the direction of feeder i. (3) The fault or overload components set.

As shown in Table 1, based on SDs, we can perceive the OP's status, security or insecurity degree. Further, with the analysis of cross security boundary corresponding to the negative SD value, we can identify fault and overload components.

D. SD-BASED PROJECTION

The state prediction variables commonly used in SA of the distribution network are load [22], voltage amplitude and phase angle [23]. After obtaining the perception information of the distribution network, it is necessary to calculate various indicators such as voltage stability index to make situation projection. However, the SD itself can be used as an indicator to measure the security level of the distribution network, of which the trends can represent the security changes. Therefore, with the SD data of the historical time, this paper uses the time-series prediction method in [22] to predict the SD in the next period of time and to achieve the prediction of the future security situation of the distribution network.

IV. CASE STUDY

A. CASE INTRODUCTION

A real 10kV distribution network of certain city core area in North China (See Fig. 4) is studied in this paper, which consists of 3 35kV/10kV substations, and 6 feeders for

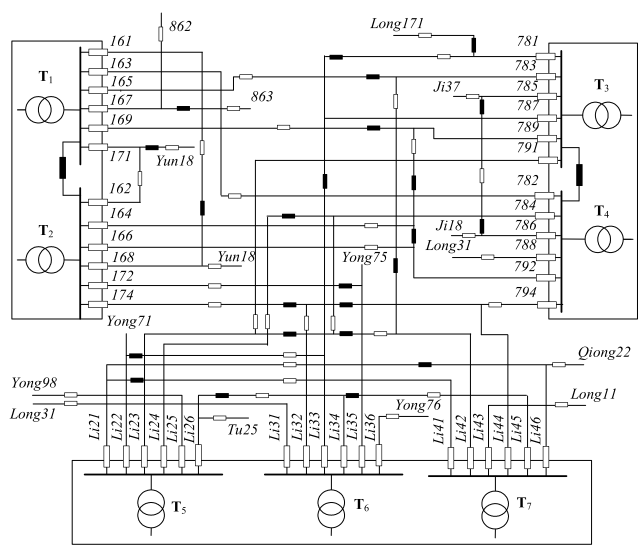

FIGURE 4. A real distribution network topology.

each transformer. The conductors of all the feeders are JKLYJ-240 with 0.125Ω/km resistance and 0.365Ω/km reactance. Table 2 shows the corresponding data of the case distribution network. The case study focuses on the operational data from 9:00 on July 1 to 8:00 on July 2, 2014, which is collected in every 1 hour.

TABLE 2. Transformers/feeders information of the case.

Substation	Transformer	Transformation ratio (kV/kV)	Capacity of transformers (MVA)	Total capacity of feeders (MVA)
S1	1#	35/10	20	47.38
	2#	35/10	20	52.37
S2	1#	35/10	20	53.69
	2#	35/10	20	54.03
S3	1#	220/35/10	20	48.84
	2#	220/35/10	20	54.55
	3#	220/35/10	20	46.93

B. CALCULATION OF SECURITY REGION AND SD

There are 42 feeders and 7 transformers in the case, hence there are 49 $N-0$ security constraints composing DSSR0; there are 66 nodes in the case, hence there are 66 groups of $N-1$ security constraints composing DSSR. The complete $N-0/N-1$ linear security boundary expressions are respectively shown in Table 5 and 6 in Appendix B.

Here we take the $N-1$ SD calculation in the direction of feeder 163 as an example to show the computation process of SD. Select the sampling data at 11:00 on July1 as the starting point $\boldsymbol{W}$. First, calculate the cross-boundary point $\boldsymbol{W}_c^*$ on the DC-Flow boundaries in the direction of feeder 163, and cross-boundary displacement $\overrightarrow{\boldsymbol{\Delta W}}^*$. The calculation result of approximate SD from $\boldsymbol{W}$ to $\boldsymbol{W}_c^*$ is 2.98MVA. Second, take $\boldsymbol{W}_c^*$ as a starting point, according to the positive or negative direction of $\overrightarrow{\boldsymbol{\Delta W}}^*$, find cross-boundary point $\boldsymbol{W}_c$ on the AC-Flow boundary using OpenDSS, then calculate the final SD. The accurate SD from $\boldsymbol{W}$ to $\boldsymbol{W}_c$ is 2.51MVA, that is the $N-1$ security margin of $\boldsymbol{W}$ at 11:00 on July 1 is 2.51MVA in the direction of feeder 163, which means the maximum increasable load of feeder 163 or its closely related feeders is 2.51MVA at this time. The detailed calculation results are shown in Table 7 in Appendix B.

C. SITUATION COMPREHENSION RESULTS

In this section, the general situation comprehension results are shown firstly, which clearly demonstrates the entire security state including all feeders' loading. Secondly, SDs in the direction of two specific feeders are selected to show the detailed situation comprehension results, including the OP trajectory in security region, SD time varying curves, fault components and guidance to dispatchers via the cross security boundary analysis.

1) GENERAL RESULTS

Calculate the $N-0/N-1$ SDs in the direction of each feeder at each time, and draw the color contour map of $N-0/N-1$ SDs to reflect the security level as shown in Fig. 5.

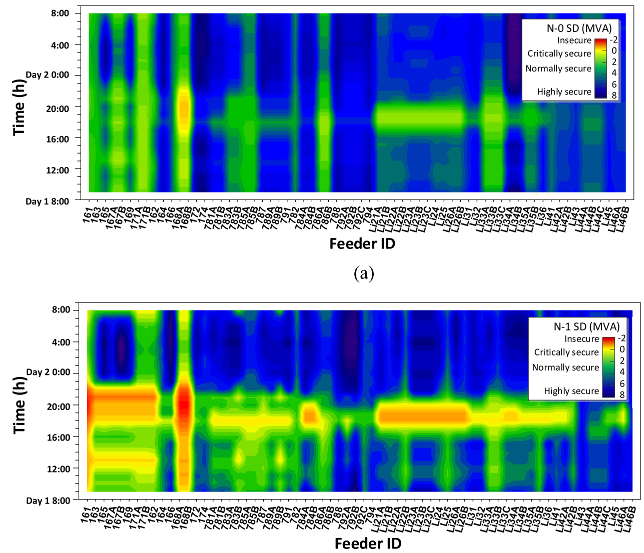

(a)

(b)

FIGURE 5. The entire security level of the case. (a) $N-0$ security level of the case. (b) $N-1$ security level of the case.

As shown in Fig. 5, the blue area corresponds to the largest SD value (about 5-8MVA), indicating a very high level of security. The green area is the next to the blue area (SD value about 1-4MVA). The SD value corresponding to the yellow area is about 0MVA, indicating that the security level is critical. The red area corresponds to a negative SD value (about (−2)-(−1) MVA), indicating insecurity.

Fig. 5(a) shows the entire $N-0$ security level of the case. Most of the area in the figure is blue, followed by green. Overall, the $N-0$ security level of the case is high. Only a very small part of the figure is dark yellow, which appears in the direction of feeders 168A and 168B during 19:00-21:00, indicating that the distribution network is in a lighter $N-0$ insecurity in this direction at this time.

Fig. 5(b) shows the entire $N-1$ security level of the case. Most of the area is blue representing the generally high level of $N-1$ security. However, the dark yellow areas are widely distributed in the direction of multiple feeders at about 11:00-13:00 and 17:00-22:00, indicating that the distribution network is lighter $N-1$ insecurity. The red areas are mostly distributed in the directions of feeders 161-162, 168A and 168B at 17:00-22:00, indicating that the distribution network is in a heavier $N-1$ insecurity level in the direction of these feeders at this time.

We make a statistical analysis of $N-0/N-1$ SDs as shown in Fig. 6, and one dot on the curve corresponds to one sampling time.

As shown in Fig. 6, (1) all dots on the average $N-0/N-1$ SD curve is located above the zero line,

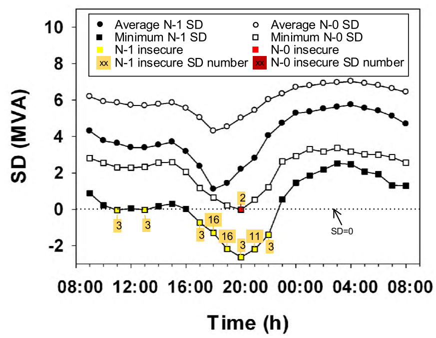

FIGURE 6. $N-0/N-1$ **SD statistical results of the case.**

showing that the entire $N-0/N-1$ security level of the case is high. (2) Only one dot (red dot) on the minimum $N-0$ SD curve is below the zero line, and the number in the red box is '2', representing $N-0$ insecurity occurs only in the direction of two feeders at 20:00, which means the $N-0$ insecurity level is relatively lighter. (3) There are 8 dots (yellow dots) on the minimum $N-1$ SD curve below the zero line, some of the number in the yellow box is larger such as '16', representing $N-1$ insecurity occurs at multiple times with multiple feeders, which means the $N-1$ insecurity level is relatively higher. In addition, the $N-1$ insecurity level is the most serious at 20:00 with the SD value −2.63 MVA.

2) DETAILED RESULTS

A feeder is arbitrarily selected in the low and heavy load area to illustrate the detailed SA comprehension results, respectively. Here we take the SD results in the direction of feeders 168A and 163 as examples.

(1) The OP trajectory.

Fig. 7 shows the OP trajectory in security region and the location relationship with the $N-0$ and $N-1$ security boundaries at different time.

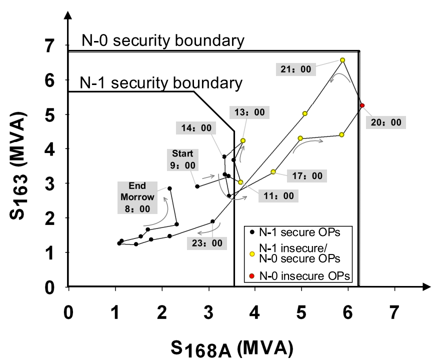

FIGURE 7. **The OP trajectory diagram.**

As shown in Fig. 7, the relative position of the OP changes with time. Starting at 9:00, it is within the $N-1$ security boundary, then it passes through the $N-1$ security boundary and becomes $N-1$ insecure for the first time at 11:00. It returns to the $N-1$ security boundary at 12:00, crosses

TABLE 3. **SDs corresponding to feeder 168A at 17:00.**

Boundary number	N-1 boundary expression	N-1 SD (MVA)
β_1	c_F^{168}-S_{161}-S_{168A}-S_{168B}=0	-0.73
β_{20}	c_F^{161}-S_{168A}-S_{161}=0	2.25
β_{21}	c_T^{1}-S_{168A}-S_{162}-S_{161}-S_{163}-S_{165}-S_{167}-S_{169}-S_{171}=0	1.02

to the $N-1$ security boundary at 13:00, then returns and crosses again to the $N-1$ security boundary. At 20:00, it crosses to $N-0$ boundary and becomes $N-0$ insecure. At 21:00, it returns to the $N-0$ security boundary and returns to the $N-1$ security boundary at 23:00 and remains $N-1$ secure until 8:00 am the next day.

In fact, since the loads on other feeders that are closely related to feeders 168A and 163 are also changing, the 2D DSSR0/DSSR size in the direction of feeders 168A and 163 is time varying. In order to display the positional relationship between the OP and the security boundaries more conveniently, we have fixed the boundaries associated with the feeders 168A and 163 during the drawing process of Fig. 7.

(2) SD time varying curve.

Based on the $N-0/N-1$ security boundaries associated with the feeders 168A and 163 (see Table 8 and 9 in Appendix B), the $N-0/N-1$ SDs of the OP at the respective time in the direction of feeders 168A and 163 are calculated, respectively (See Table 10 and 11 in Appendix B). A SD time varying line chart is illustrated in Fig. 8.

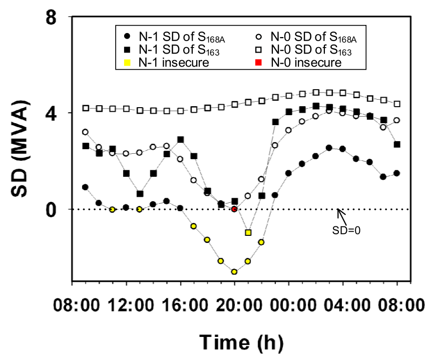

FIGURE 8. $N-0/N-1$ **SD curves in the direction of feeders 168A and 163.**

The red color in Fig. 8 represents a negative $N-0$ SD, and the yellow color represents that the $N-1$ SD is negative. In the direction of feeder 168A, the $N-1$ SDs are negative at a plurality of times such as 11:00, 13:00 and 17:00-22:00 (see yellow dots), and even the $N-0$ SD is negative at 20:00 (see the red dot). In the direction of feeder 163, the $N-1$ SD is negative only at 21:00 (see the yellow square), and the $N-0$ SDs at every moment are positive.

(3) SD-based situation comprehension results

We illustrate the comprehension of the SDs by taking two OPs of which the $N-1$ SD is respectively positive and negative in the direction of feeder 168A.

TABLE 4. Predicted $N-0/N-1$ security statistical results of the case.

Prediction time(h)	N-0 insecure feeder number	N-0 insecure feeder ratio	Average N-0 SD(MVA)	Minimum N-0 SD(MVA)	N-1 insecure feeder number	N-1 insecure feeder ratio	Average N-1 SD(MVA)	Minimum N-1 SD(MVA)
Day2 9:00	0	0	6.54	2.84	0	0	4.34	1.08
10:00	0	0	6.38	2.78	0	0	4.21	0.45
11:00	0	0	6.19	2.02	3	4.55%	3.81	-0.46
12:00	0	0	6.11	1.88	3	4.55%	3.64	-0.49

TABLE 5. The complete $N-0$ linear security boundary expressions of the case.

Boundary number	Linear expression	Boundary number	Linear expression
β_1^0	c_F^{161}-S_{161}=0	β_{26}^0	c_F^{792}-S_{792}=0
β_2^0	c_F^{163}-S_{163}=0	β_{27}^0	c_F^{794}-S_{794}=0
β_3^0	c_F^{165}-S_{165}=0	β_{28}^0	c_T^4-S_T^4=0
β_4^0	c_F^{167}-S_{167}=0	β_{29}^0	c_F^{li21}- S_{li21}=0
β_5^0	c_F^{169}-S_{169}=0	β_{30}^0	c_F^{li22}- S_{li22}=0
β_6^0	c_F^{171}-S_{171}=0	β_{31}^0	c_F^{li23}- S_{li23}=0
β_7^0	c_T^1-S_T^1=0	β_{32}^0	c_F^{li24}- S_{li24}=0
β_8^0	c_F^{162}-S_{162}=0	β_{33}^0	c_F^{li25}- S_{li25}=0
β_9^0	c_F^{164}-S_{164}=0	β_{34}^0	c_F^{li26}- S_{li26}=0
β_{10}^0	c_F^{166}-S_{166}=0	β_{35}^0	c_T^5-S_T^5=0
β_{11}^0	c_F^{168}-S_{168}=0	β_{36}^0	c_F^{li31}- S_{li31}=0
β_{12}^0	c_F^{172}-S_{172}=0	β_{37}^0	c_F^{li32}- S_{li32}=0
β_{13}^0	c_F^{174}-S_{174}=0	β_{38}^0	c_F^{li33}- S_{li33}=0
β_{14}^0	c_T^2-S_T^2=0	β_{39}^0	c_F^{li34}- S_{li34}=0
β_{15}^0	c_F^{781}-S_{781}=0	β_{40}^0	c_F^{li35}- S_{li35}=0
β_{16}^0	c_F^{783}-S_{783}=0	β_{41}^0	c_F^{li36}- S_{li36}=0
β_{17}^0	c_F^{785}-S_{785}=0	β_{42}^0	c_T^6-S_T^6=0
β_{18}^0	c_F^{787}-S_{787}=0	β_{43}^0	c_F^{li41}- S_{li41}=0
β_{19}^0	c_F^{789}-S_{789}=0	β_{44}^0	c_F^{li42}- S_{li42}=0
β_{20}^0	c_F^{791}-S_{791}=0	β_{45}^0	c_F^{li43}- S_{li43}=0
β_{21}^0	c_T^3-S_T^3=0	β_{46}^0	c_F^{li44}- S_{li44}=0
β_{22}^0	c_F^{782}-S_{782}=0	β_{47}^0	c_F^{li45}- S_{li45}=0
β_{24}^0	c_F^{784}-S_{784}=0	β_{48}^0	c_F^{li46}- S_{li46}=0
β_{24}^0	c_F^{786}-S_{786}=0	β_{49}^0	c_T^7-S_T^7=0
β_{25}^0	c_F^{788}-S_{788}=0		

At 17:00, the specific SDs between the OP and the corresponding security boundaries in the direction of feeder 168A are shown in Table 3.

As shown in Table 3, the violated $N-1$ security boundary is β_1: c_F^{168}-S_{161}-S_{168A}-S_{168B} =0 at 17:00, and the $N-1$ SD is -0.73 MVA. This indicates that the load on feeder 168A, or the load on the closely related feeders (the feeder appearing in the expression of β_1, 161,168B) needs to reduce the load by at least 0.73 MVA to meet $N-1$ security. The reason for this violation is that the fault of feeder 161 causes the capacity of feeder 168A to be overloaded. Therefore, we can analyze that at the current moment, the fault components include feeder 161, and the overload components include feeder 168A with an overload of 0.73 MVA.

Similarly, at 23:00 the $N-1$ SD in the direction of feeder 168A is 0.56 MVA (See Table 11 in Appendix B). This indicates that the load on feeder 168A, or its closely related feeders can increase the maximum power by 0.56 MVA.

(4) Guidance providing to dispatchers based on SD.

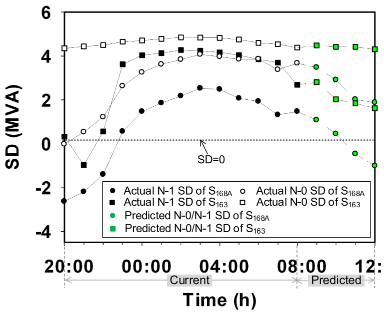

FIGURE 9. SD prediction results in the direction of feeders 168A and 163.

As shown in Fig. 8, in the direction of feeder 168A the $N-0$ SD is -0.02 MVA at 20:00. The distribution network is in an emergency state at this time, and the dispatcher must take certain measures, such as cutting off at least 0.02MVA load in feeder 168A, to restore the distribution network to normal operation state; at other times, the $N-0$ SD is positive. The $N-1$ SDs are smaller than 0 at multiple times, indicating that the distribution network is often in an $N-1$ insecurity state, so the dispatcher should pay more attention to feeder 168A. In the direction of feeder 163, the $N-0/N-1$ SDs at all times are larger than 0, so there is less need for the focus on feeder 163 from the dispatcher.

In summary, since the SD in the direction of feeder 168A appears negative and the SD in the direction of feeder 163 remains positive, the dispatcher should focus on tracking feeder 168A, then taking measures to cut or reduce the load at the right time.

D. SITUATION PROJECTION RESULTS

1) THE ENTIRE SECURITY PREDICTION RESULTS

Since the SD trends can represent the security state trends of the distribution network, this paper uses the time series based prediction method in [22] to project the future security situation of the distribution network based on the SDs of historical moments. The entire security prediction results of the case are shown in Table 4.

It can be seen from the Table 4 that in the next 4 hours, the $N-0$ SD of the distribution network shows a downward trend, but it remains positive; the $N-1$ SD also shows a downward trend, but it may appear to be negative.

2) THE DETAILED SECURITY PREDICTION RESULTS

We take the SD prediction in the direction of feeders 168A and 163 as an example. According to the calculated SDs in

TABLE 6. The complete $N-1$ linear security boundary expressions of the case.

Boundary number	Linear expression	Boundary number	Linear expression
β_1	c_F^{168}-S_{161}-S_{168A}-S_{168B}=0	β_{59}	c_F^{164}- S_{792C} - S_{164} =0
β_2	c_T^2-S_{161} -S_T^2-S_{171A}=0	β_{60}	c_T^2- S_{792C} -S_T^2- S_{792B} =0
β_3	c_F^{782}-S_{163} -S_{782}=0	β_{61}	c_F^{li44}- S_{794} - S_{li44} =0
β_4	c_T^2-S_{163} -S_T^4=0	β_{62}	c_T^7- S_{794} -S_T^7=0
β_5	c_F^{783}-S_{165} - S_{783} =0	β_{63}	c_F^{li46}- S_{li21A} - S_{li46} =0
β_6	c_T^3- S_{165} - S_{169} -S_T^3=0	β_{64}	c_T^7- S_{li21A} - S_{li23C} -S_T^7- S_{li21B}=0
β_7	c_F^{863}- S_{167A} - S_{863} =0	β_{65}	c_F^{li41}- S_{li21B} - S_{li41} =0
β_8	c_F^{862}- S_{167B} - S_{862} =0	β_{66}	c_T^7- S_{li21B} - S_{li23C} -S_T^7- S_{li21A}=0
β_9	c_F^{162}- S_{171A} - S_{162} =0	β_{67}	c_F^{784}-S_{li23A} -S_{784}=0
β_{10}	c_T^2- S_{171A} - S_{161}-S_T^2=0	β_{68}	c_T^4-S_{li23A}-S_{li24} -S_T^4=0
β_{11}	c_F^{yun18}- S_{171B} - S_{yun18} =0	β_{69}	c_F^{791}-S_{li23B} -S_{791}=0
β_{12}	c_F^{789}- S_{169} - S_{789} =0	β_{70}	c_T^3-S_{li23B} -S_T^3=0
β_{13}	c_T^3-S_{169} -S_{165} -S_T^3=0	β_{71}	c_F^{li42}-S_{li23C} -S_{li42}=0
β_{14}	c_F^{171}-S_{162} -S_{171}=0	β_{72}	c_T^7-S_{li23C} -S_{li21A} -S_T^7- S_{li21B}=0
β_{15}	c_T^1-S_{162} -S_T^1-S_{168A}=0	β_{73}	c_F^{li33}-S_{li22A} -S_{li33}=0
β_{16}	c_F^{792}-S_{164} -S_{792}=0	β_{74}	c_T^6-S_{li22A} -S_{li26A} -S_T^6=0
β_{17}	c_T^4-S_{164} -S_T^4 -S_{166}=0	β_{75}	c_F^{yong71}-S_{li22B} - S_{yong71}=0
β_{18}	c_F^{792}-S_{166} -S_{792}=0	β_{76}	c_F^{784}-S_{li24} -S_{784}=0
β_{19}	$c_{T,max}^4$-S_{166} -S_{164} - S_T^4=0	β_{77}	c_T^4-S_{li24} -S_{li23A} -S_T^4=0
β_{20}	c_F^{161}-S_{168A} -S_{161}=0	β_{78}	c_F^{yong98}-S_{li25} - S_{yong98}=0
β_{21}	c_T^1-S_{168A} -S_{162}-S_T^1=0	β_{79}	c_F^{li34}-S_{li26A} -S_{li34}=0
β_{22}	c_F^{yun18}-S_{168B} -S_{yun18}=0	β_{80}	c_T^6-S_{li26A} -S_{li22A} -S_T^6=0
β_{23}	c_F^{li35}-S_{172} -S_{li35}=0	β_{81}	c_F^{tu25}-S_{li26B} -S_{tu25}=0
β_{24}	c_T^6-S_{172} -S_T^6=0	β_{82}	c_F^{long31}-S_{li31} -S_{long31}=0
β_{25}	c_F^{li44}-S_{174} -S_{li44}=0	β_{83}	c_F^{li44}-S_{li32} -S_{li44}=0
β_{26}	c_T^7-S_{174} -S_T^7=0	β_{84}	c_T^7-S_{li32} -S_{li34B} -S_T^7=0
β_{27}	c_F^{li33}-S_{781A} -S_{li33}=0	β_{85}	c_F^{781}-S_{li33A} -S_{781}=0
β_{28}	c_T^6-S_{781A} -S_T^6 -S_{787}=0	β_{86}	c_T^3-S_{li33A} -S_T^3=0
β_{29}	c_F^{long31}-S_{781B} - S_{long31}=0	β_{87}	c_F^{782}-S_{li33B} -S_{782}=0
β_{30}	c_F^{li42}-S_{783A} -S_{li42}=0	β_{88}	c_T^4-S_{li33B} -S_T^4=0
β_{31}	c_T^7-S_{783A} -S_T^7=0	β_{89}	c_F^{li22}-S_{li33C} -S_{li22}=0
β_{32}	c_F^{165}-S_{783B} -S_{165}=0	β_{90}	c_T^5-S_{li33C} -S_{li34A} -S_T^5=0
β_{33}	c_T^1-S_{783B} -S_{789B} -S_T^1=0	β_{91}	c_F^{li26}-S_{li34A} -S_{li26}=0
β_{34}	c_F^{786}-S_{785A} -S_{786}=0	β_{92}	c_T^5-S_{li34A} -S_{li33C} -S_T^5=0
β_{35}	c_T^4-S_{785A} -S_{789A} -S_T^4=0	β_{93}	c_F^{li45}-S_{li34B} -S_{li45}=0
β_{36}	c_F^{ji37}-S_{785B} -S_{ji37}=0	β_{94}	c_T^7-S_{li34B} -S_{li32} -S_T^7=0
β_{37}	c_F^{li33}-S_{787} -S_{li33}=0	β_{95}	c_F^{172}-S_{li35A} -S_{172}=0
β_{38}	c_T^6-S_{787} -S_{781A} -S_T^6=0	β_{96}	c_T^2-S_{li35A} -S_T^2=0
β_{39}	c_F^{792}-S_{789A} -S_{792}=0	β_{97}	c_F^{yong75}-S_{li35B} - S_{yong75}=0
β_{40}	c_T^4-S_{789A} -S_{785A} -S_T^4=0	β_{98}	c_F^{yong76}-S_{li36} - S_{yong76}=0
β_{41}	c_F^{169}-S_{789B} -S_{169}=0	β_{99}	c_F^{li21}-S_{li41} -S_{li21}=0
β_{42}	c_T^1-S_{789B} -S_{783B} -S_T^1=0	β_{100}	c_T^5-S_{li41} -S_{li42A} -S_{li46A} - S_T^5=0
β_{43}	c_F^{li23}-S_{791} -S_{li23}=0	β_{101}	c_F^{li23}-S_{li42A} -S_{li23}=0
β_{44}	c_T^5-S_{791} -S_T^5=0	β_{102}	c_T^5-S_{li42A} -S_{li41} -S_{li46A} - S_T^5=0
β_{45}	c_F^{163}-S_{782} -S_{163}=0	β_{103}	c_F^{783}-S_{li42B} -S_{783}=0
β_{46}	c_T^1-S_{782} -S_T^1=0	β_{104}	c_T^3-S_{li42B} -S_T^3=0
β_{47}	c_F^{li23}-S_{784A} -S_{li23}=0	β_{105}	c_F^{long11}-S_{li43} -S_{long11}=0
β_{48}	c_T^5-S_{784A} -S_T^5-S_{784B}=0	β_{106}	c_F^{174}-S_{li44A} -S_{174}=0
β_{49}	c_F^{li24}-S_{784B} -S_{li24}=0	β_{107}	c_T^2-S_{li44A} -S_T^2=0
β_{50}	c_T^5-S_{784B} -S_T^5 -S_{784A}=0	β_{108}	c_F^{794}-S_{li44B} -S_{794}=0
β_{51}	c_F^{785}-S_{786A} -S_{785}=0	β_{109}	c_T^4-S_{li44B} -S_T^4=0
β_{52}	c_T^3-S_{786A} -S_T^3 -S_{792A}=0	β_{110}	c_F^{li32}-S_{li44C} -S_{li32}=0
β_{53}	c_F^{ji18}-S_{786B} -S_{ji18}=0	β_{111}	c_T^6-S_{li44C} -S_T^6-S_{li45}=0
β_{54}	c_F^{long31}-S_{788} -S_{long31}=0	β_{112}	c_F^{li32}-S_{li45} -S_{li32}=0
β_{55}	c_F^{789}-S_{792A} -S_{789}=0	β_{113}	c_T^6-S_{li45} -S_T^6 -S_{li44C}=0
β_{56}	c_T^3-S_{792A} -S_T^3 -S_{786A}=0	β_{114}	c_F^{li21}-S_{li46A} -S_{li21}=0
β_{57}	c_F^{166}-S_{792B} -S_{166}=0	β_{115}	c_T^5-S_{li46A} -S_{li42A} -S_{li41} - S_T^5=0
β_{58}	c_T^2-S_{792B} -S_T^2 -S_{792C}=0	β_{116}	$c_F^{qiong22}$-S_{li46B} - $S_{qiong22}$=0

the direction of feeders 168A and 163, the SD change trend in the next 4 hours is predicted as shown in Fig. 9.

TABLE 7. Results about $N-1$ sd in the direction of feeder 163.

Starting point ***W***	(2.48,1.84,0.83,0.82,1.52,3.09,1.49,1.83,1.20,2.34,0.28,2.35,1.45,0.82,1.56,1.15,1.50,1.67,1.71,0.30,1.61,2.34,0.27,1.28,0.28,1.24,0.28,1.91,1.43,0.87,0.92,0.89,1.28,0.03,0.81,1.19,1.21,0.22,2.36,0.81,0.27,0.22,2.50,2.43,2.20,0.25,1.36,0.28,2.10,1.22,0.80,0.82,1.30,1.77,1.01,0.81,0.69,0.12,1.42,1.11,0.92,0.17,1.10,0.88,0.44,0.94)^T
Cross-boundary point W_c^* on DC-Flow boundary	(2.48,**4.82**,0.83,0.82,1.52,3.09,1.49,1.83,1.20,2.34,0.28,2.35,1.45,0.82,1.56,1.15,1.50,1.67,1.71,0.30,1.61,2.34,0.27,1.28,0.28,1.24,0.28,1.91,1.43,0.87,0.92,0.89,1.28,0.03,0.81,1.19,1.21,0.22,2.36,0.81,0.27,0.22,2.50,2.43,2.20,0.25,1.36,0.28,2.10,1.22,0.80,0.82,1.30,1.77,1.01,0.81,0.69,0.12,1.42,1.11,0.92,0.17,1.10,0.88,0.44,0.94)^T
Approximate SD W to W_c^*	2.98 (MVA)
Cross-boundary point W_c on AC-Flow boundary	(2.48,**4.35**,0.83,0.82,1.52,3.09,1.49,1.83,1.20,2.34,0.28,2.35,1.45,0.82,1.56,1.15,1.50,1.67,1.71,0.30,1.61,2.34,0.27,1.28,0.28,1.24,0.28,1.91,1.43,0.87,0.92,0.89,1.28,0.03,0.81,1.19,1.21,0.22,2.36,0.81,0.27,0.22,2.50,2.43,2.20,0.25,1.36,0.28,2.10,1.22,0.80,0.82,1.30,1.77,1.01,0.81,0.69,0.12,1.42,1.11,0.92,0.17,1.10,0.88,0.44,0.94)^T
Accurate SD W to W_c	2.51 (MVA)

TABLE 8. $N-0$ linear security boundaries corresponding to feeders 168A and 163.

Feeder ID	Boundary number	Linear expression
168A	β_{11}^0	c_F^{168}-S_{168A}-S_{168B}=0
	β_{14}^0	c_T^2-S_{162}-S_{164}-S_{166}-S_{168A}-S_{168B}-S_{172}-S_{174}=0
163	β_2^0	c_F^{163}-S_{163} =0
	β_7^0	c_T^1-S_{161}-S_{163}-S_{165}-S_{167}-S_{169}-S_{171}=0

TABLE 9. $N-1$ linear security boundaries corresponding to feeders 168A and 163.

Feeder ID	Boundary number	Linear expression
168A	β_1	c_F^{168}-S_{161}-S_{168A}-S_{168B} =0
	β_{20}	c_F^{161}-S_{168A} -S_{161}=0
	β_{21}	c_T^1-S_{168A} -S_{162}-S_{161}-S_{163}-S_{165}-S_{167}-S_{169}-S_{171}=0
163	β_3	c_F^{782}-S_{163} -S_{782} =0
	β_4	c_T^2-S_{163} -S_T^4=0
	β_{21}	c_T^1-S_{168A} -S_{162}-S_{161}-S_{163}-S_{165}-S_{167}-S_{169}-S_{171}=0

It can be seen from Fig. 9 that the $N-0/N-1$ SD in the direction of feeders 168A and 163 in the next 4 hours

TABLE 10. $N-0$ security distance at each time.

Time (h)	SD of Feeder 168A (MVA)	SD of Feeder 163 (MVA)	Time (h)	SD of Feeder 168A (MVA)	SD of Feeder 163 (MVA)
Day1 9:00	3.18	4.20	21:00	0.53	4.44
10:00	2.55	4.18	22:00	1.22	4.50
11:00	2.31	4.17	23:00	2.63	4.65
12:00	2.29	4.17	Day2 0:00	3.26	4.71
13:00	2.33	4.10	1:00	3.62	4.79
14:00	2.56	4.09	2:00	3.84	4.85
15:00	2.60	4.08	3:00	4.07	4.84
16:00	2.06	4.08	4:00	3.97	4.83
17:00	1.18	4.14	5:00	3.85	4.75
18:00	0.65	4.21	6:00	3.86	4.60
19:00	0.21	4.24	7:00	3.38	4.54
20:00	**-0.02**	4.35	8:00	3.67	4.38

TABLE 11. $N-1$ security distance at each time.

Time (h)	SD of Feeder 168A (MVA)	SD of Feeder 163 (MVA)	Time (h)	SD of Feeder 168A (MVA)	SD of Feeder 163 (MVA)
Day1 9:00	0.89	2.63	21:00	**-2.19**	**-0.97**
10:00	0.23	2.33	22:00	**-1.40**	0.56
11:00	**-0.04**	2.51	23:00	0.56	3.62
12:00	0.05	1.49	Day2 0:00	1.47	4.04
13:00	**-0.03**	0.64	1:00	1.86	4.13
14:00	0.18	1.49	2:00	2.18	4.28
15:00	0.31	2.29	3:00	2.53	4.24
16:00	0.02	2.89	4:00	2.48	4.17
17:00	**-0.73**	2.21	5:00	2.07	4.04
18:00	**-1.30**	0.76	6:00	1.93	3.85
19:00	**-2.18**	0.19	7:00	1.32	3.70
20:00	**-2.63**	0.33	8:00	1.47	2.69

shows a downward trend, but the $N-0$ SD does not appear to be a negative value temporarily. The $N-1$ SD may be negative in the direction of feeder 168A, but the $N-1$ SD still remains positive in the direction of feeder 163. Therefore, the dispatcher should focus more on tracking the load changes of feeder 168A to prevent insecurity or even urgency.

V. CONCLUSION

Situation awareness (SA) plays an important role in security monitoring and control of the distribution network operation. In this paper, distribution system security region (DSSR) is applied to SA for the first time, and a novel security distance (SD) based security SA method is proposed. The contribution of the proposed method is as follows.

(1) It inherits the advantages of the region methodology, avoids complex iterative operations and reduces the computation, and considers the $N-0$ security and $N-1$ security of distribution networks simultaneously.

(2) It presents a color contour map, which can clearly visualize the entire SA results in three dimensions of time, space and security. The higher the security of distribution networks, the wider the blue area distribution in the color contour map; conversely, the lower the security, the wider the yellow area distribution, and even the red area.

(3) It can determine whether an operating point (state) is $N-0/N-1$ secure and calculate the degree of security or insecurity. For negative SD scenarios, the fault or overload components set can be recognized via cross security boundary analysis.

(4) It can predict the security level of distribution networks in the near future.

With the help of the proposed method, feeders with SDs that remains short for a long period or that would be reduced by prediction, or that the dispatchers are concerned with, can be chosen to monitor their SDs trend to prevent undesirable situations. The method in this paper is suitable for tracking and predicting the secure status in real time in distribution network operation. In further research, emerging components such as DGs and DER will be taken into account in the proposed method.

APPENDIX

A. AC-FLOW MODEL OF DSSR AND DSSR0

The DSSR model considering network loss and voltage constraints is established in [17], which is formulated as:

$$\boldsymbol{\Omega}_{\text{DSSR}} = \{\boldsymbol{W} \in \boldsymbol{\Theta} | f(\boldsymbol{V}, \boldsymbol{\theta}) = \boldsymbol{W}, g_{N-1}(\boldsymbol{W}) \le 0\} \quad \text{(A1)}$$

where $\boldsymbol{\Theta}$ is the state space, $f(\boldsymbol{V}, \boldsymbol{\theta}) = \boldsymbol{W}$ are the power flow equations, $g_{N-1}(\boldsymbol{W}) \le 0$ are the security constraints after $N-1$ contingency, formulated as:

$$\begin{cases} S_F^m = \sum_{n=1} S_{F,tr}^{m,n} + Loss_m \\ S_{F,tr}^{n,m} + \sum_{m=1} S_{F,tr}^{m,n} + Floss_{nm} \le c_F^m \\ S_{T,tr}^{u,v} = \sum_{m \in T_u, n \notin T_v} (\sum_{n=1} S_{F,tr}^{m,n} + Loss_n) \\ S_{T,tr}^{u,v'} = \sum_{m \in T_u, n \in T_v} (S_{F,tr}^{m,n} + \sum_{m=1} S_{F,tr}^{n,m} + Floss_{mn}) \\ S_{T,tr}^{u,v} + S_{T,tr}^{u,v'} \le c_T^v \\ V_i^m \le V_i \le V_i^M \end{cases} \quad \text{(A2)}$$

where S_F^m is the power measured at the outlet of feeder m; $S_{F,tr}^{m,n}$ is the load transferred from feeder m to feeder n; $Loss_m$ is the network loss under normal operation state. $Floss_{nm}$ is the power loss of feeder m when an $N-1$ fault occurs at the outlet of n and its load is transferred to m; c_F^m is the thermal capacity of feeder m. $S_{T,tr}^{u,v}$ is the sum of power flow at the outlet of feeders which derive from transformer v but don't connect with transformer u when an $N-1$ fault occurs at u. $S_{T,tr}^{u,v'}$ is the sum of power flow at the outlet of feeders which derive from transformer v and connect with transformer u when an $N-1$ fault occurs at u. c_T^v is the rated capacity of transformer v. V_i^m and V_i^M are the lower and upper limits of node voltage amplitude, respectively.

DSSR0 can be formulated as:

$$\boldsymbol{\Omega}_{\text{DSSR0}} = \{\boldsymbol{W} \in \boldsymbol{\Theta} | f(\boldsymbol{V}, \theta) = \boldsymbol{W}, g_{N-0}(\boldsymbol{W}) \le 0\} \quad \text{(A3)}$$

where $g_{N-0}(\boldsymbol{W}) \leq 0$ are security constraints satisfied in normal operation of distribution networks, including the capacity constraints of feeders and substation transformers, as well as the constraints of the voltage drop of nodes, formulated as:

$$\begin{cases} S_F^m = \sum\limits_{n=1} S_{F,tr}^{m,n} + Loss_m \\ S_F^m \leq c_F^m \\ S_T^u = \sum\limits_{m \in T_u} (\sum\limits_{n=1} S_{F,tr}^{m,n} + Loss_m) \\ S_T^u \leq c_T^u \\ V_i^m \leq V_i \leq V_i^M \end{cases} \tag{A4}$$

where S_T^u is the sum of power flow at the outlet of feeders which derive from transformer u.

B. OTHER ANALYSIS RESULTS OF THE CASE

See Tables 5–11.

REFERENCES

[1] S.-Z. Chen *et al.*, "An aerodynamics-based novel optimal power extraction strategy for offshore wind farms with central VSCs," *IEEE Access*, vol. 6, pp. 44351–44361, Dec. 2018.
[2] M. R. Endsley, B. Bolté, and D. G. Jones, *Designing for Situation Awareness: An Approach to User-Centered Design*. New York, NY, USA: Taylor and Francis, 2003.
[3] E. S. Connors, M. R. Endsley, and L. Jones, "Situation awareness in the power transmission and distribution industry," in *Proc. Hum. Factors Ergon. Soc. Annu. Meeting*, Oct. 2007, vol. 51, no. 4, pp. 215–219.
[4] M. R. Endsley and E. S. Connors, "Situation awareness: State of the art," in *Proc. IEEE Power and Energy Soc. Gen. Meeting, Convers. Del. Elect. Energy 21st Century*, Aug. 2008, pp. 1–4.
[5] J. A. Wischkaemper, C. L. Benner, B. D. Russell, and K. Manivannan, "Application of waveform analytics for improved situational awareness of electric distribution feeders," *IEEE Trans. Smart Grid*, vol. 6, no. 4, pp. 2041–2049, Apr. 2015.
[6] J. Wu, K. Ota, M. Dong, J. Li, and H. Wang, "Big data analysis-based security situational awareness for smart grid," *IEEE Trans. Big Data*, vol. 4, no. 3, pp. 408–417, Sep. 2016.
[7] C. S. Chen Sun, D. L. Dong Liu, and Y. W. Yun Wang, "Operation situational awareness based on dynamic power flow for a profound analysis of active distribution network," in *Proc. CIRED Workshop*, Helsinki, Finland, 2016, pp. 36–38.
[8] E. Lakervi and E. J. Holmes, *Electricity Distribution Network Design*, 2nd ed. London, U.K.: IET, 2003.
[9] J. Xiao, W. Gu, C. Wang, and F. Li, "Distribution system security region: Definition, model and security assessment," *IET Gener. Transm. Distrib.*, vol. 6, no. 10, pp. 1029–1035, Oct. 2012.
[10] T. Yang and Y. Yu, "Static voltage security region-based coordinated voltage control in smart distribution grids," *IEEE Trans. Smart Grid*, vol. 9, no. 6, pp. 5494–5502, Nov. 2018.
[11] C. Wan, J. Lin, W. Guo, and Y. Song, "Maximum uncertainty boundary of volatile distributed generation in active distribution network," *IEEE Trans. Smart Grid*, vol. 9, no. 4, pp. 2930–2942, Jul. 2018.
[12] S. Clegg and P. Mancarella, "Integrated modeling and assessment of the operational impact of power-to-gas (P2G) on electrical and gas transmission networks," *IEEE Trans. Sustain. Energy*, vol. 6, no. 4, pp. 1234–1244, Oct. 2015.
[13] J. Xiao, G. Zu, X. Gong, and F. Li, "Observation of security region boundary for smart distribution grid," *IEEE Trans. Smart Grid*, vol. 8, no. 4, pp. 1731–1738, Jul. 2017.
[14] Z. Gu, X. Jun, and S. Kai, "Mathematical base and deduction of security region for distribution systems with DER," *IEEE Trans. Smart Grid*, to be published. doi: 10.1109/TSG.2018.2814584.
[15] J. Xiao, G. Zu, Q. He, X. Tan, X. Li, and G. Zhen, "Empirical analysis on distribution system security region," (in Chinese), *Autom. Elect. Power Syst.*, vol. 41, no. 3, pp. 153–160, Feb. 2017. doi: 10.7500/AEPS20160617008.
[16] J. Xiao, B.-Q. Zhang, G.-Q. Zu, G.-D. Zhen, J.-C. Xiao, and Q.-S. Lin, "Two kinds of security distance for distribution network," in *Proc. IEEE Power Energy Soc. Gen. Meeting*, Chicago, IL, USA, Jul. 2017, pp. 1–5.
[17] J. Xiao, L. Zuo, G. Zu, and S. Liu, "Model of distribution system security region based on power flow calculation," (in Chinese), *Proc. CSEE*, vol. 37, no. 17, pp. 4941–4949, Sep. 2017. doi: 10.13334/j.0258-8013.pcsee.161733.
[18] J. Liu, H. Cheng, P. Zeng, and L. Yao, "Rapid assessment of maximum distributed generation output based on security distance for interconnected distribution networks," *Int. J. Electr. Power Energy Syst.*, vol. 101, pp. 13–24, Oct. 2018.
[19] G. Zu, J. Xiao, and K. Sun, "Distribution network reconfiguration comprehensively considering N-1 security and network loss," *IET Gener. Transmiss. Distrib.*, vol. 12, no. 8, pp. 1721–1728, Jun. 2018.
[20] J. Liu, H. Cheng, Y. Tian, P. Zeng, and L. Yao, "Stochastic multi-objective distribution feeder reconfiguration based on point estimation considering N-1 security and net loss," in *Proc. IEEE Power Energy Soc. Gen. Meeting*, Boston, MA, USA, 2016, pp. 1–5.
[21] J. Xiao, B. Zhang, and M. Zhang, "The formation of distribution network security boundaries," (in Chinese), *Proc. CSEE*, vol. 37, no. 20, pp. 5922–5932, Jul. 2017. doi: 10.13334/j.0258-8013.pcsee.161938.
[22] N. Amjady, "Short-term hourly load forecasting using time-series modeling with peak load estimation capability," *IEEE Trans. Power Syst.*, vol. 16, no. 3, pp. 498–505, Aug. 2001.
[23] M. Huang, Z. Wei, G. Sun, Y. Sun, H. Zang, and K. W. Cheung, "A historical data-driven unscented kalman filter for distribution system state estimation," in *Proc. IEEE Power Energy Soc. Gen. Meeting*, Chicago, IL, USA, Jul. 2017, pp. 1–5.

JUN XIAO received the Ph.D. degree in electrical engineering from Tianjin University, China, in 2003, where he is currently a Professor of planning and evaluation of urban power supply grid and a Ph.D. Tutor. His research interests include power supply capability of distribution networks, distribution system security region, planning and evaluation of distribution networks, and smart grid.

BAOQIANG ZHANG received the M.S. degree from the School of Mechanical Engineering, Tianjin University, Tianjin, China, in 2013, where he is currently pursuing the Ph.D. degree with the School of Electrical and Information Engineering. His research interests include distribution system security region, and smart distribution systems planning and assessment.

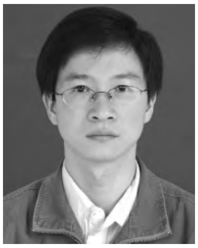

FENGZHANG LUO received the B.Eng., M.Eng., and Ph.D. degrees from Tianjin University, Tianjin, China, in 2003, 2006, and 2010, respectively. His research interests include (active) distribution system planning and decision making, and artificial intelligence application in power systems.